

# PERFORMANCE ANALYSIS OF 6 SLOT 8 POLE PERMANENT MAGNET LINEAR MOTOR

F. Azhar<sup>1\*</sup>, M. Norhisam<sup>2</sup>, H. Wakiwaka<sup>3</sup>,  
K. Tashiro<sup>4</sup>, M. Nirei<sup>5</sup>

<sup>1,3,4</sup>Faculty of Engineering, Shinshu University, 4-17-1,  
Wakasato, Nagano, 380-8553 Japan

<sup>2</sup>Faculty of Engineering, Universiti Putra Malaysia,  
43400, Serdang, Malaysia

<sup>5</sup>Department of Electronic and Computer Science,  
Nagano National College of Technology,  
716, Takuma, Nagano, 381-8550 Japan

## ABSTRACT

*Currently, palm oil is the most consumed vegetable oil in the world. Therefore, an increment in its productivity is essential to ensure its sustainability in the market. One option is through the mechanization of the tools used to harvest it. In this paper, the design of the actuator for mechanized oil palm harvesting tools was discussed. A 3 phase permanent magnet linear motor with a 6 slot 8 pole structure topology known as 3PhSTLOA was used as the actuator structure. The structure of 3PhSTLOA has been optimized. The aim of the optimization is to allow the 3PhSTLOA to produce at least 200 N of average thrust at a total weight of under 2.0 kg. As a result of optimizing the 3PhSTLOA produced about 202 N of average thrust at 1.8 kg of its total weight. The performance of 3PhSTLOA is then compared with the previous type of actuator in mechanized harvesting tools.*

**KEYWORDS:** *Electrical time constant; Thrust characteristics; Slot type; Permanent magnet linear motor*

## 1.0 INTRODUCTION

Mechanization has been proven as a way to improve agricultural productivity. (Asoegwu & Asoegwu, 2007). The same technique was applied to palm oil fresh fruit bunch (FFB) harvesting tools in order to enhance harvesting productivity (Abdul Razak et al., 2008; Azhar et al., 2012a). In Malaysia, efforts to mechanize FFB harvesting tools has been initiated by the Malaysian Palm Oil Board (MPOB) through

---

\* Corresponding author email: fairul.azhar@utem.edu.my

development of a tool named *Cantas*<sup>TM</sup>. Based on field trials, it was found that the *Cantas*<sup>TM</sup> improved productivity of palm oil 3 times compared to traditional tools (Abdul Razak et al., 2008). However, due to operational limitations of *Cantas*<sup>TM</sup>, this tool performs inefficiently at oil palms more than 8 meters tall (Abdul Razak et al., 2008; Azhar et al., 2012a). Therefore, a new type of FFB harvesting tool called the E-Cutter was proposed (Azhar, 2009). Detailed construction and operation of both FFB harvesting tools is explained in Azhar et al., (2012a).

The progress of E-Cutter development depends on electrical generator and linear motor design and development progress. While the design and development of an electrical generator seems to be established as discussed in Norhisam et al., (2011), the design and development of a linear motor are still in progress. Previously, a single phase permanent magnet slot type of linear motor has been designed and developed in Azhar et al., (2011). The structure and thrust characteristics of this linear motor, known as 1PhSTLOA is as shown in Figure 1. The 1PhSTLOA was designed based on a target starting thrust,  $F_x=0\text{mm}$  of 200 N. The aimed starting thrust,  $F_x=0\text{mm}$  was determined based on the required cutting force during FFB harvesting activity as discussed in Abdul Razak et al., (2008). On top of that, in order to ensure the reliability of the E-Cutter, the 1PhSTLOA is designed to have a total weight of 2.0 kg.

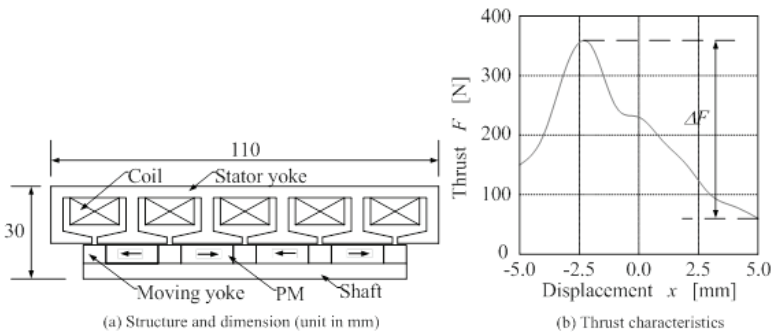


Figure 1. Structure and thrust characteristics of 1PhSTLOA

The 1PhSTLOA has been fabricated and underwent testing in order to prove its functionality. Based on the test results, it was determined that FFB harvesting was feasible. However, the performance of the 1PhSTLOA need to be improved especially in terms of mover speed (Azhar et al., 2012b). By increasing the mover speed, the overall harvesting cycle time of FFB will decrease thus resulting in an incremental increase in productivity. Therefore, a new linear motor design for the E-Cutter was needed.

## 1.0 CONSIDERATION OF DESIGNING LINEAR MOTOR FOR E-CUTTER

In order to improve overall performance of the E-Cutter, linear motor improvements need to be done. The focus will be given to the mover response of the linear motor. Mover response of the linear motor is related to the electrical time constant,  $\tau_e$  which can be calculated using Equation (1). The electrical time constant,  $\tau_e$  needs to be as small as possible to realize a high speed response in the linear motor (Mizuno et al., 2000).

$$\tau_e = \frac{L}{R} \quad (1)$$

where  $\tau_e$  is the electrical time constant in [ms],  $L$  is the coil inductance in [mH] and  $R$  is the coil resistance in [ $\Omega$ ].

The 1PhSTLOA has a total displacement of 10 mm and an oscillation frequency,  $f_{osc}$  of 68 Hz. The new linear motor aims to have a total displacement of 20 mm and an oscillation frequency,  $f_{osc}$  of 80 Hz. This target is set by comparing to the *Cantas*<sup>TM</sup> which has these performance characteristics (Abdul Razak et al., 2008).

Despite the mover response, the new linear motor also needs a required thrust characteristics. As presented in Azhar, (2009), the average thrust,  $F_{ave}$  should be higher than 200 N. In Azhar et al., (2011), the 1PhSTLOA has been designed and developed to fulfill this thrust requirement. However, the 1PhSTLOA produced a high thrust ripple,  $\Delta F$  of about 300 N as shown in Figure 1 (b). In order to ensure smooth operation of the linear motor, the thrust ripple,  $\Delta F$  needed to be reduced (Lee & Kim, 2006).

A 3 phase structure has been proven to reduce thrust ripple,  $\Delta F$ . By controlling the excitation sequence of a 3 phase coil, the thrust ripple,  $\Delta F$  can be reduced even though a balanced 3 phase supply is used. Also, in the 3 phase structure, the number of coils energized for each phase will be reduced compared to a similar total coil number and size in a single phase structure. This could help reduce the total inductance,  $L$  for each phase and hence reduce the electrical time constants,  $\tau_e$  of the linear motor. Furthermore, the displacement and motion direction are relatively easy to control by controlling the 3 phase supply sequence (Azhar et al., 2012b). The new linear motor will be called as 3PhSTLOA to differentiate it from previous models of a linear motor for the

### E-Cutter.

Nowadays, there are various types of permanent magnets so magnetization direction has been proposed. From a simple N-S arrangement either in the axial direction (Zhu et al., 1997; Kim & Bryan, 2004) or the radial direction (Jang et al., 2003; Nakaiwa et al., 2011) to the halbach array (Wang & Howe, 2005; Nakaiwa et al., 2011). Despite these magnetization directions, the halbach array is found to have the capability to control magnetic flux path direction and increase efficiency (Nakaiwa et al., 2011). Therefore, the halbach array is used in the 3PhSTLOA.

Based on the considerations mentioned above, the structure of the 3PhSTLOA is as shown in Figure 2. It uses a 6 slot 8 pole 3 phase structure configuration. The permanent magnet magnetic pitch,  $\tau_{pm}$  has been set to 24 mm while the coil pitch,  $\tau_c$  has been set to 16 mm. The length of the air gap,  $\delta$  was set to 0.5 mm and the yoke thickness,  $t_y$  was set to 2 mm.

The structural dimensions of the 3PhSTLOA need to be optimized in order to achieve the desired thrust. On top of that, the total weight,  $W$  of the 3PhSTLOA needs to be below 2.0 kg in order to ensure reliability of the E-Cutter. In the optimization, the height of the permanent magnet (PM),  $h_{pm}$  and the coil,  $h_c$  varied within a fixed total radius,  $r_{total}$  and restricted weight,  $W$  in order to obtain the highest average thrust,  $F_{ave}$ . Initially, the shaft radius,  $r_s$  was set to 1 mm and the total radius,  $r_{total}$  was set to 20 mm, 25 mm and 30 mm. The input power,  $P_{in}$  for each model was fixed at 100 W per phase.

Meanwhile, due to various values used for the height of the PM,  $h_{pm}$  and coil,  $h_c$ , some of the structural parameters will change accordingly such as coil turns,  $N$ , coil resistance,  $R$  and total weight,  $W$ . The height of the PM,  $h_{pm}$  has been varied with a starting value of 1 mm. The PM height,  $h_{pm}$  was increased by 1 mm until it reached its maximum value within the fixed total radius,  $r_{total}$ . At the same time, the height of the coil,  $h_c$ , coil turns,  $N$ , coil resistance,  $R$  and total weight,  $W$  were changed accordingly and were calculated using Equations (2) - (6).

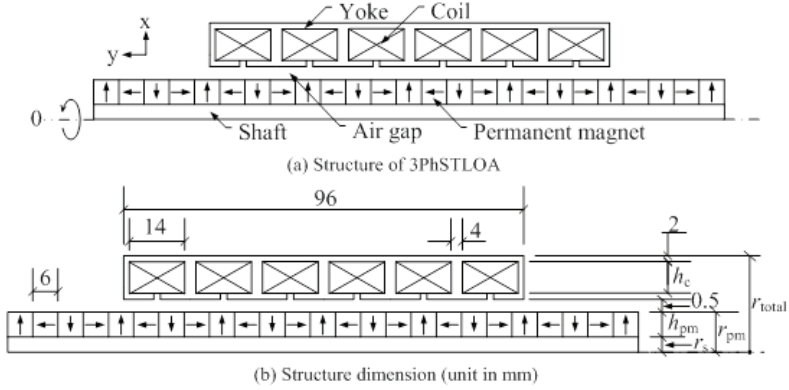


Figure 2. Linear motor for E-Cutter (3PhSTLOA)

$$h_c = r_{total} - (r_s + h_{pm} + \delta + 2t_y) \quad (2)$$

$$N = \frac{W_c}{\phi_C} \times \frac{h_c}{\phi_C} \quad (3)$$

$$R = \zeta N^2 \frac{\sigma l}{a} \quad (4)$$

$$= \zeta \left( \frac{W_c}{\phi_C} \times \frac{h_c}{\phi_C} \right)^2 \frac{8\pi\sigma \left( r_s + h_{pm} + \delta + t_y + \frac{h_c}{2} \right)}{\pi\phi_C^2}$$

$$I_{in} = \sqrt{\frac{P_{in}}{R}} \quad (5)$$

$$= \sqrt{\frac{100}{R}}$$

$$W = \rho_{copper} v_{coil} + \rho_{NdFeB} v_{PM} + \rho_{S45C} v_{yoke} + \rho_{SUS304} v_{shaft} \quad (6)$$

where  $h_c$  is the height of coil in [m],  $r_{total}$  is the total radius in [m],  $r_s$  is the shaft radius in [m],  $h_{pm}$  is the height of the PM in [m],  $\delta$  is the air gap length in [m],  $t_y$  is the yoke thickness in [m],  $N$  is the number of coil turns,  $W_c$  is the width of the coil in [m],  $\phi_C$  is the copper wire diameter in [m],  $R$  is the coil resistance in [ $\Omega$ ],  $\zeta$  is the coil space factor,  $\sigma$  is the copper resistivity in [ $\Omega \cdot m$ ],  $I_{in}$  is the input current in [A],  $P_{in}$  is the input power in [W],  $W$  is the total weight in [kg],  $\rho_{material}$  is the material density in [ $kg/m^3$ ] and  $v_{parts}$  is the part volume in [ $m^3$ ].

Once the optimized structure of the 3PhSTLOA with the highest average thrust,  $F_{ave}$  within the restricted weight,  $W$  is obtained, the shaft radius,  $r_s$  was increased within the fixed outer radius of the PM,  $r_{pm}$ .

While the shaft radius,  $r_s$  was increased, the thrust of the 3PhSTLOA was observed. This step is essential in order to strengthen the structure of the 3PhSTLOA. Therefore, a shaft radius,  $r_s$  that does not affect the thrust will be proposed for final fabrication.

### 3.0 DESIGN OF 3PhSTLOA

#### 3.1 Structure Optimization for High Thrust and Light Weight Performance Charactersitics

Dynamic thrust characteristics were used to evaluate the 3PhSTLOA. A 3 phase power supply has been used in the simulation with a frequency of 70 Hz. At that frequency a mover oscillation frequency of 80 Hz will be obtained. Based on dynamic thrust characteristics, the average thrust,  $F_{ave}$  was calculated and compared for each model.

Figure 3 shows the dynamic thrust characteristics of the 3PhSTLOA at several total radius  $r_{total}$ . Based on the thrust characteristics of all 3PhSTLOA models, the average thrust,  $F_{ave}$  was calculated. On top of that, the total weight of each 3PhSTLOA model was also calculated.

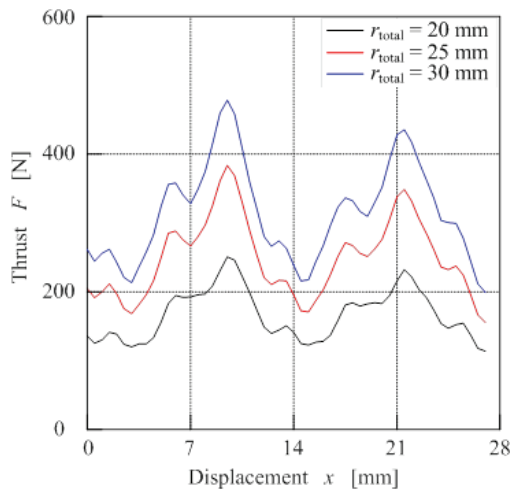


Figure 3. Thrust characteristics of linear actuator with different of total radius,  $r_{total}$

Figure 4 shows the effect of the PM outer radius,  $r_{pm}$  on the average thrust,  $F_{ave}$  and the total weight,  $W$  of 3PhSTLOA. As shown in Figure 4, the value of average thrust,  $F_{ave}$  increases as the PM outer radius,  $r_{pm}$  increases until it reaches a maximum value before starting to decrease. The thrust value decreases exceeding this point even though the PM outer radius,  $r_{pm}$  increases since the height of the coil,  $h_c$  decreases. It

will cause the number of coil turns to decrease and will minimize the value of the magneto motive force in the coil.

On the other hand, the total weight of the 3PhSTLOA is only influenced by the total radius,  $r_{total}$ . This is because the bigger the total radius,  $r_{total}$  of the 3PhSTLOA, the bigger the size of the coil and causes a higher value of coil material density compared to the other material. Thus coil size will most directly influence the total weight of 3PhSTLOA.

The 3PhSTLOA models that have the highest average thrust,  $F_{ave}$  at every total radius,  $r_{total}$  are identified and summarized in Table 1. As shown in Table 1, the 3PhSTLOA with a total radius,  $r_{total}$  of 25 mm and 30 mm fulfil the average thrust,  $F_{ave}$  requirement with values of 250 N and 316 N respectively. On the other hand, the 3PhSTLOA with total radius,  $r_{total}$  of 20 mm and 25 mm fulfil the total weight,  $W$  restrictions of 1.13 kg and 1.80 kg respectively.

Therefore, the structure of the 3PhSTLOA with a total radius,  $r_{total}$  of 25.0 mm was selected as the initial model. It has an average thrust,  $F_{ave}$  of 250 N and a total weight,  $W$  of 1.8 kg at an input power of 100 W per phase. On top of that, the outer radius of the PM  $r_{pm}$  of this model is 13 mm and the height of the coil,  $h_c$  is 7.5 mm. Figure 5 shows the effect of an excitation current to 3PhSTLOA's thrust characteristics. This model has a shaft radius,  $r_s$  of 1 mm. The shaft radius,  $r_s$  was increased by 1 mm up to within the fixed outer radius of the PM,  $r_{pm}$ . The purpose of this step is to increase the strength of the 3PhSTLOA structure. The excitation current,  $I$  was varied from 0 A up to 3 A.

Figure 6 shows the effect of shaft radius,  $r_s$  to the 3PhSTLOA average thrust,  $F_{ave}$  at several excitation currents,  $I$ . Based on this figure, the reduction in average thrust,  $F_{ave}$  is not significant to shaft radius,  $r_s$  below 6 mm. For shaft radius,  $r_s$  higher than 6 mm, the 3PhSTLOA's average thrust,  $F_{ave}$  was significantly reduced. Therefore, a shaft radius,  $r_s$  of 6 mm is considered as the optimized dimension.

The final dimension for the 3PhSTLOA structure is as shown in Figure 7. It has 462 coil turns with 14.2  $\Omega$  of winding resistance for each coil and about a similar total weight,  $W$  with the initial structure. Figure 8 shows the effect of the excitation current,  $I_p$  to the 3PhSTLOA's thrust characteristics. Since there is a reduction in terms of the permanent magnet size, therefore, the thrust characteristics of the final 3PhSTLOA structure are therefore lower when compared to Figure 5 within the same excitation current. It needs about 125 W per phase to be supplied in order to achieve the targeted average thrust,  $F_{ave}$  which is 200 N compared with only 93 W in the initial structure.

Table 1. Average thrust,  $F_{ave}$  and total weight,  $W$  of optimized model of each  $r_{total}$

No.	Total radius, $r_{total}$ (mm)	PM outer radius, $r_{pm}$ (mm)	Average thrust, $F_{ave}$ (N)	Total weight, $W$ (kg)
1	20.0	10	178	1.13
2	25.0	13	250	1.80
3	30.0	15	316	2.62

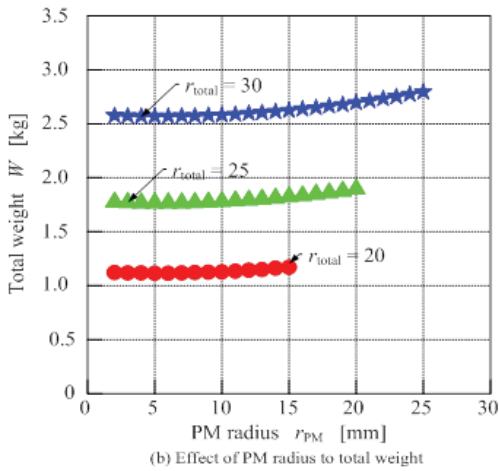
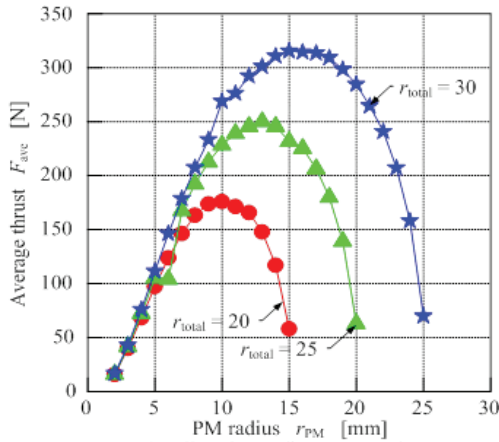


Figure 4. Average thrust  $F_{ave}$  and total weight,  $W$  of 3PhSTLOA

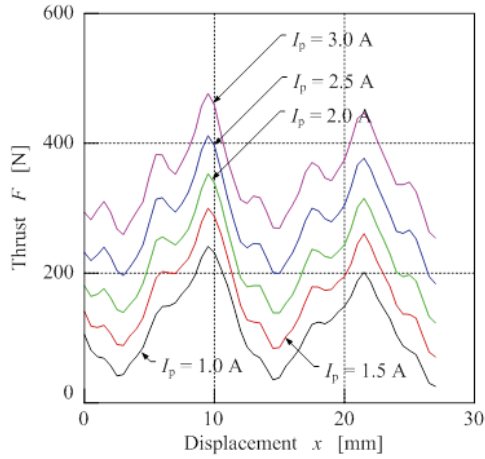


Figure 5. Effect of excitation current to thrust characteristics of 3PhSTLOA

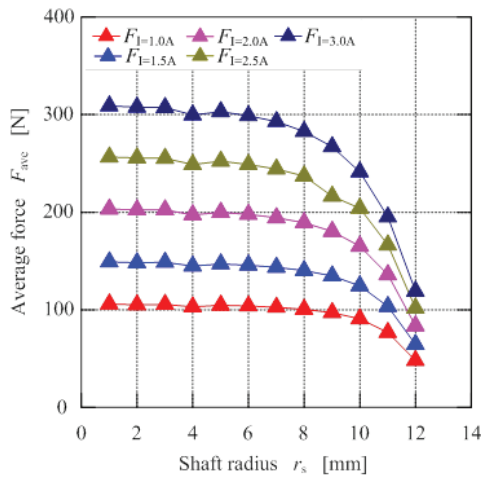


Figure 6. Effect of shaft radius,  $r_s$  to average thrust,  $F_{ave}$  of 3PhSTLOA

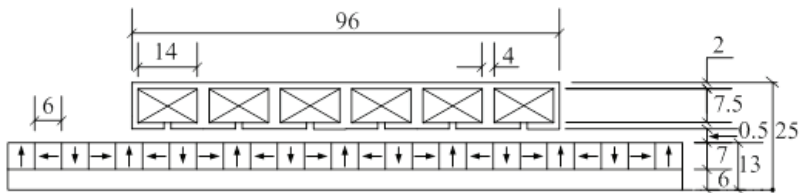


Figure 7. Final structure dimension of 3PhSTLOA (unit:mm)

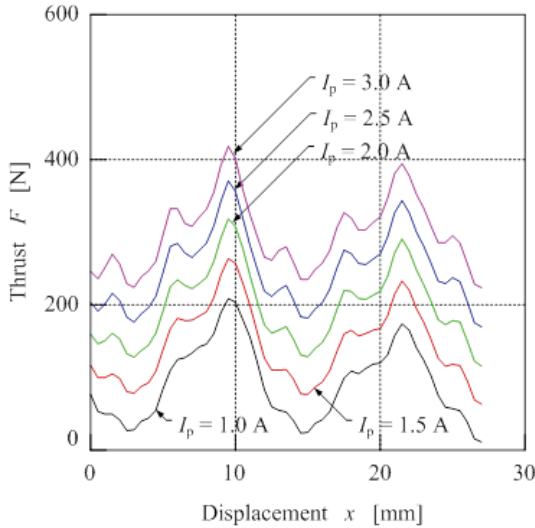


Figure 8. Effect of excitation current to thrust characteristics of final 3PhSTLOA's structure

### 3.2 Electrical Time Constant Calculation of 3PhSTLOA

The electrical time constant,  $\tau_e$  of the 3PhSTLOA needs to be as low as possible in order to mode the current response faster. Since the 3PhSTLOA was excited at 70 Hz by a 3 phase power supply, the electrical time constant,  $\tau_e$  of the 3PhSTLOA should be less than half of the excitation cycle time which is 7.14 ms in order to allow the excitation current to reach its maximum value before the next voltage half cycle starts.

The inductance,  $L$  of the 3PhSTLOA was estimated by its voltage and current waveform. Figure 9 shows the excitation waveform of the 3PhSTLO and based on this the time when the voltage and current are zero,  $t_v$  and  $t_i$  were identified as shown in figure 9 (b). The electrical time constant,  $\tau_e$  was calculated using equation (1). Therefore, the coil resistance,  $R$  and the inductance,  $L$  need to be estimated. This can be done using Equations (7) and (8).

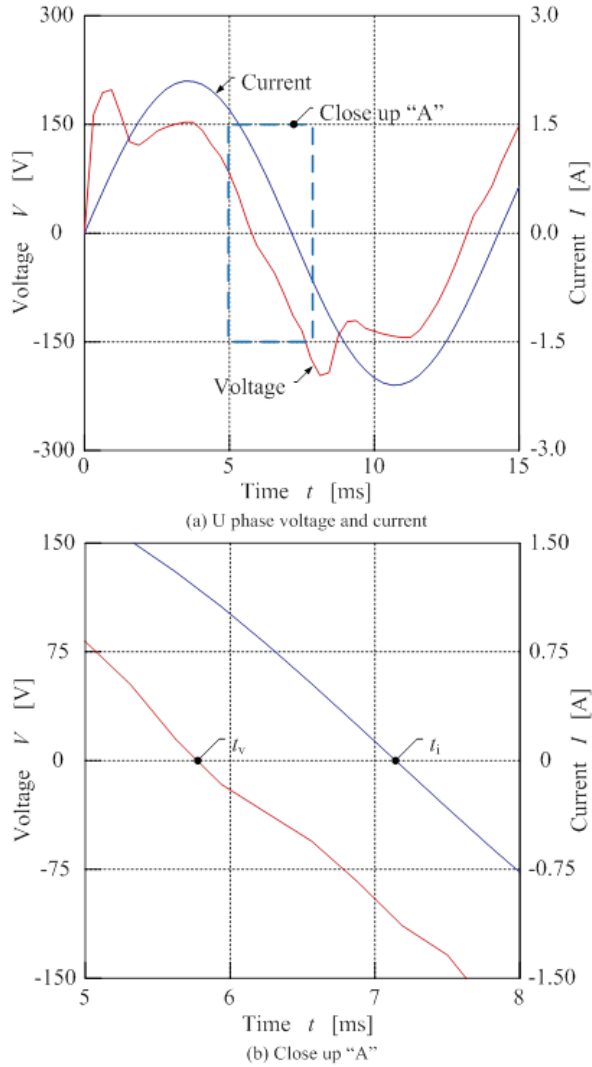


Figure 9. Excitation Waveform

$$R = \frac{V_{rms}}{I_{rms}} \sin(2\pi f [t_i - t_v]) \tag{7}$$

$$L = \frac{V_{rms} / I_{rms} \cos(2\pi f [t_i - t_v])}{2\pi f} \tag{8}$$

Where  $R$  is the coil resistance in  $[\Omega]$ ,  $V_{rms}$  is the RMS excitation voltage in  $[V]$ ,  $f$  is the excitation frequency in  $[Hz]$ ,  $t_i$  is the time excitation current and is 0 A in  $[s]$ ,  $t_v$  is the time excitation voltage and is 0 V in  $[s]$  and  $L$  is the coil inductance in  $[H]$ .

Based on the excitation voltage and current waveform and equations (7) and (8) the coil resistance,  $R$  was estimated to be about  $72.90 \Omega$  and the coil inductance,  $L$  was estimated to be about  $115.74 \text{ mH}$ . Therefore, the electrical time constant,  $\tau_e$  of the 3PhSTLOA was estimated to be about  $1.58 \text{ ms}$  which is lower when compared to the target value. This confirms the earlier hypothesis that this kind of structure topology could reduce the inductance due to a reduction in the number of coils excited per phase in the 3PhSTLOA when compared to a 1PhSTLOA. In the 3PhSTLOA, 2 coils with a total of 654 coil turns are excited for each phase compared to the 1PhSTLOA, 5 coils with a total of 2450 coil turns are excited simultaneously.

#### 4.0 PERFORMANCE COMPARISON OF 3PhSTLOA AND 1PhSTLOA

The performance of the 3PhSTLOA was compared to the 1PhSTLOA. The comparison of thrust characteristics between their linear actuators is as shown in figure 10. It can be seen that the 1PhSTLOA has a higher maximum thrust compared to the 3PhSTLOA with about  $380 \text{ N}$  and  $310 \text{ N}$  respectively. However, the minimum thrust of the 3PhSTLOA is higher compared to 1PhSTLOA at about  $140 \text{ N}$  and  $40 \text{ N}$  respectively. This proves that the 3PhSTLOA has a reduced thrust ripple compared to the 1PhSTLOA of  $170 \text{ N}$  and  $340 \text{ N}$  respectively.

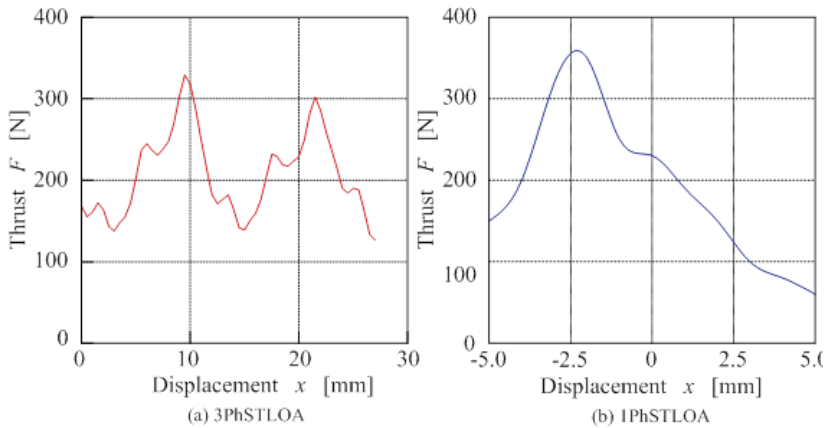


Figure 10. Thrust characteristics of 3PhSTLOA and 1 PhSTLOA

The performance of the 3PhSTLOA is then compared to 1PhSTLOA using other performance characteristics. There are the thrust constant,  $k_f$ , the motor constant,  $k_m$  and the motor constant square density,  $G$ . These performance characteristics can be calculated using equations (9) to (11).

$$k_f = \frac{F}{I} \quad (9)$$

$$k_m = \frac{F}{\sqrt{P_{in}}} \quad (10)$$

$$G = \frac{F^2}{P_{in}V} \quad (11)$$

where  $k_f$  is the thrust constant in [N/A],  $F$  is the average thrust for the 3PhSTLOA and the starting thrust for the 1PhSTLOA in [N],  $I$  is the excitation current in [A],  $k_m$  is the motor constant in [N/ $\sqrt{W}$ ],  $P_{in}$  is the input power in [W],  $G$  is the motor constant square density in [N<sup>2</sup>/Wm<sup>3</sup>] and  $V$  is the actuator volume in [m<sup>3</sup>].

The performance comparison of the 3PhSTLOA and the 1PhSTLOA is as shown in table 2. In order to make a valid comparison, the maximum thrust,  $F_{max}$  was chosen instead of average thrust,  $F_{ave}$  or starting thrust,  $F_{x=0mm}$ . Based on table 2, both 3PhSTLOA and 1PhSTLOA have similar values for the motor constant,  $k_m$ . It shows that both the 3PhSTLOA and 1PhSTLOA are capable of producing similar thrust at the same input power. However, in the other performance characteristics, the 3PhSTLOA shows better performance compared to 1PhSTLOA. The thrust constant,  $k_f$  shows the capability of the 3PhSTLOA to produce double thrust at a similar excitation current,  $I$  compared to the 1PhSTLOA. Furthermore, by referring to the motor constant square density,  $G$ , the structure topology of the 3PhSTLOA has the capability to produce higher thrust at a lower size and input power compared to the 1PhSTLOA. For these reasons, the 3PhSTLOA is shown to have better performance compared to the 1PhSTLOA. On top of this, the 3PhSTLOA also has a lower electrical time constant,  $\tau_e$  compared to the 1PhSTLOA. Therefore, the 3PhSTLOA response is estimated higher when compared to the 1PhSTLOA.

Table 2. Performance comparison of 3PhSTLOA and 1PhSTLOA

No.	Performance characteristics	3PhSTLOA	1PhSTLOA
1	Thrust constant, $k_f$ (N/A)	226.95	103.54
2	Motor constant, $k_m$ (N/ $\sqrt{W}$ )	28.62	28.32
3	Motor constant square density, $G$ ( $\times 10^6$ N <sup>2</sup> /Wm <sup>3</sup> )	4.36	2.55
4	Electrical time constant, $\tau_e$ (ms)	1.58	3.71

## 5.0 CONCLUSION

The design of a linear motor for the E-Cutter has been discussed. Previously, the 1PhSTLOA was designed for the E-Cutter. It has a starting thrust,  $F_{x=0 \text{ mm}}$  of about 222 N and an oscillation frequency,  $f_{\text{osc}}$  of 68 Hz. The 1PhSTLOA has been tested to prove its functionality. However, its oscillation frequency,  $f_{\text{osc}}$  needs to be improved in order to increase cutting speed. For this reason the 3PhSTLOA was designed. The structure of the 3PhSTLOA has been optimized in order to achieve higher thrust at a restricted weight level. The result is the 3PhSTLOA which has an average thrust,  $F_{\text{ave}}$  of 202 N at 125 W of input power,  $P_{\text{in}}$ . The performance comparison of the 3PhSTLOA to the 1PhSTLOA has also been discussed. It was found that, the 3PhSTLOA has better performance compared to 1PhSTLOA. Therefore, it was demonstrated that the 3PhSTLOA is able to be implemented as the E-Cutter actuator.

## 6.0 ACKNOWLEDGEMENT

F. Azhar wishes to acknowledge the Universiti Teknikal Malaysia Melaka (UTeM), and Ministry of Higher Education of Malaysia, for giving him the opportunity to pursue his PhD study and for their financial support of Shinshu University.

## 7.0 REFERENCES

- Abdul Razak J., Desa A., Ahmad H., Azmi Y. & Johari J. (1999). Reaction force and energy requirements for cutting oil palm fronds by spring powered sickle cutter. *Journal of Oil Palm Research*, 11(2), 114-122.
- Abdul Razak J, Ahmad H., Johari J., Malik N., Yosri G. & Omar A. (2008). CantasTM - A tool for the efficient harvesting of oil palm fresh fruit bunches. *Journal of Oil Palm Research*, 20, 548 – 558.
- Asoegwu, S. N. & Asoegwu A.O. (2007). An overview of agricultural mechanization and its environmental management in Nigeria. *Agricultural Engineering International: the CIGR Journal*, 9(6), 1-22.
- Azhar F. (2009). *Design of a linear oscillatory actuator for oil palm mechanical cutter* (Unpublished master's thesis). University Putra Malaysia, Selangor, Malaysia.
- Azhar F., Norhisam M., Mailah N.F., Zare M.R., Wakiwaka H. & Nirei M. (2011). Thrust Optimization of Linear Oscillatory Actuator Using Permeance Analysis Method. *International Review of Electrical Engineering (I.R.E.E.)*, 6(7) 2929 – 2938.

- Azhar F., Norhisam M., Wakiwaka H., Tashiro K. & Nirei M. (2012a). Current Achievement and Future Plan for Improvement for E Cutter Development. *The 24<sup>th</sup> Symposium on Electromagnetics and Dynamics, SEAD 24*, 459-464.
- Azhar F., Norhisam M., Wakiwaka H., Tashiro K. & Nirei M. (2012b). Initial progress and possible improvement of E-Cutter linear actuator development, *IEEE International Conference on Power and Energy*, 933-938.
- Kim W.J., & Bryan C.M. (2004). Development of a Novel Direct-Drive Tubular Linear Brushless Permanent-Magnet Motor. *International Journal of Control, Automation and Systems*, 2(3), 279-288.
- Lee D.Y. & Kim G.T. (2006). Design of thrust ripple minimization by equivalent magnetizing current considering slot effect, *IEEE Transactions on Magnetics*, 42 (4), 1367 - 1370.
- Mizuno T., Iwadare M., Nanahara M., Koyama K., Anzai T., Nirei M. & Yamada H. (2000). Considerations on electrical and mechanical time constants of a moving-magnet-type linear DC motor. *Sensors and Actuators 81*, 301-304.
- Nakaiwa K., Wakiwaka H., Tashiro K. (2011). Thrust Characteristics Comparison of Interior Magnet Type Pencil Size Cylinder Linear Motor. *Journal of the Japan Society of Applied Electromagnetics and Mechanics*, 19(3), 509 -512.
- Norhisam M., Norafiza M., Azhar F., Mailah N.F., Wakiwaka H. & Nirei M. (2011). Optimization of Pole Numbers and Rotor Size for a Single Phase Slot-less Permanent Magnet Generator. *International Review of Electrical Engineering (I.R.E.E.)*, 6(5), 2253 – 2260.
- Wang J. & Howe D. (2005). Tubular Modular Permanent-Magnet Machines Equipped With Quasi-Halbach Magnetized Magnets—Part I: Magnetic Field Distribution, EMF, and Thrust Force. *IEEE Transactions on Magnetics*, 41(9), 2470 – 2478.
- Zhu Z. Q., Horward P. J., Howe D. & Rees-Jones J. (1997). Calculation of Cogging Force in a Novel Slotted Linear Tubular Brushless Permanent Magnet Motor. *IEEE Transactions on Magnetics*, 33(5), 4098 – 4100.

